Int. J. of Applied Mechanics and Engineering, 2006, vol.11, No.4, pp.965-979

MODELING AND STRESS ANALYSIS OF NOZZLE CONNECTIONS IN ELLIPSOIDAL HEADS OF PRESSURE VESSELS UNDER EXTERNAL LOADING

V.N. SKOPINSKY* and A.B. SMETANKIN
Moscow State Industrial University
Avtozavodskaya 16, 115280 Moscow, RUSSIA
e-mail: skopin-j@mail.msiu.ru

This paper presents the structural modeling and stress analysis of nozzle connections in ellipsoidal heads subjected to external loadings. Timoshenko shell theory and the finite element method are used. The features of the structural modeling of ellipsoid-cylinder shell intersections, numerical procedure and SAIS special-purpose computer program are discussed. A parametric study of the effects of geometric parameters on the maximum effective stresses in the ellipsoid-cylinder intersections under loading was performed. The results of the stress analysis and parametric study of the nozzle connections are presented.

Key words: ellipsoidal head; nozzle connections; finite element method; stress concentration; external forces and moments.

1. Introduction

Pressure vessels are widely applied in many branches of industry such as chemical and petroleum machine-building, nuclear and power engineering, gas, oil and oil-refining industries, aerospace techniques, etc. Welded nozzles connecting a pressure vessel to piping can be placed both on the cylindrical shell and the heads of the vessel. Cylindrical nozzles and ellipsoidal heads are often used in practice. Geometrical parameters of nozzle connections may significantly vary even in one pressure vessel.

One of the parts of the overall structural analysis for nozzle connections in the ellipsoidal head is the stress analysis of two intersecting shells. Due to different loadings applied to these structures, a local stress state of the nozzle connection characterized by high stress concentrations occurs in the intersection region. Internal pressure is the primary loading used in the structure analysis for determination of main vessel-nozzle dimensions (at the designing phase). However, the effect of external forces and moments applied to the nozzle should be taken into consideration in addition to the stresses caused by the internal pressure. External loadings usually are imposed by a piping system attached to the nozzle. Values of the loads and moments are calculated by an analysis of the piping system.

Many works including analytical, experimental and numerical investigations have been devoted to the stress analysis of nozzle connections in pressure vessels subjected to different external loadings. However, most of these works were related to the nozzle connections in cylindrical or spherical shells. Certain aspects of this problem were disscused by Bijlaard (1955; 1957), Darevskiy (1964), Gill (1970) and other authors. The Welding Research Council (WRC) Bulletins 107, 297 and 326 (Wichman *et al*., 1965; 1979; Mershon *et al*., 1984; 1987) provide empirical methods for calculating stresses at the vessel-nozzle junction which has been widely used by design analysts.

The problem of ellipsoidal-cylinder shell intersections has not been investigated sufficiently. Most of the works published have been limited to the ellipsoidal heads with a radial central nozzle. An approximate analytical method of influence coefficients (Galletly, 1959; 1960) was used in order to study the stress concentration at reinforced openings in ellipsoidal heads under internal pressure loading. Chao *et al*. (1985a;b;c; 1986) presented an analytical study and results of parametric analysis for nozzles in pressure

---

* To whom correspondence should be addressed

vessel heads under internal pressure and axial load. Approximate methods for evaluation of peak stresses under the internal pressure were considered in Zemel and Fedenko (1974) and Mashel (1977). In previous works of Skopinsky *et al*. (1994; 2000; 2003) the results of a parametric study of the ellipsoidal head with non-radial and non-central nozzles under internal pressure loading were presented.

The purpose of the present paper is to further investigate the ellipsoidal-cylinder shell intersections subjected to external loading for a better understanding of this problem.

2. Ellipsoid-cylinder intersections

Stress analysis of the nozzle connection in an ellipsoidal pressure vessel head is a complex problem. Application of numerical method is the most common and effective approach to solving this problem. In this analysis, the nozzle connection is considered as an intersection of two shells (Skopinsky and Berkov, 1994): the ellipsoidal shell of revolution (basic shell) and cylindrical shell (nozzle). It is an adequate model of this shell structure which allows taking into account geometry complexity and features of an elastic interaction between shells.

For the ellipsoidal-cylinder intersection, two typical planes are selected. These planes pass through the normal $\boldsymbol{n_0}$ to the ellipsoid surface at the point of the intersection of this surface by the nozzle axis (Fig.1). The main plane passes through the axis of the basic shell and the normal $\boldsymbol{n_0}$. The transverse plane is perpendicular to the main one.

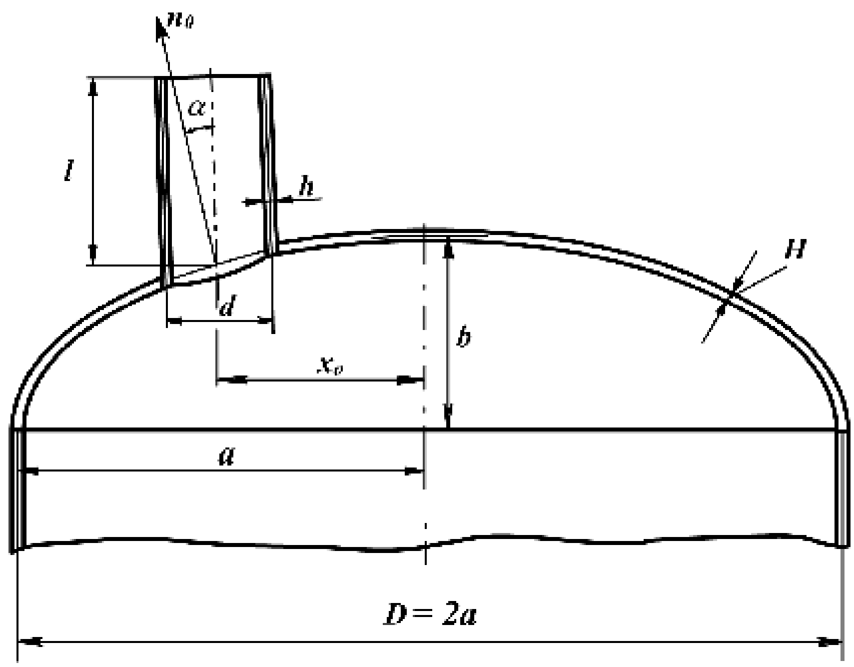

Fig.1. Ellipsoidal head and nozzle shell intersection geometry.

The parameter $\bar{x}_0$ defines the relative offset nozzle displacement from the central position, the parameter α defines the angular deflection from the radial position (from the normal $\boldsymbol{n_0}$ to the head shell surface).

With the purpose of a systematic parametric analysis the following typical nozzle connections in ellipsoidal head are considered: central $(\bar{x}_0 = 0)$, non-central $(\bar{x}_0 \neq 0)$; radial $(\alpha = 0)$ and non-radial $(\alpha \neq 0)$ (Fig.2).

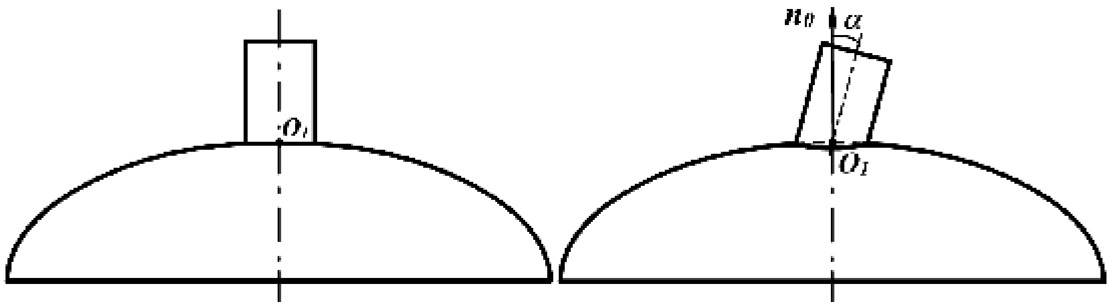

radial connection non-radial connection

a) ellipsoidal head with central nozzle

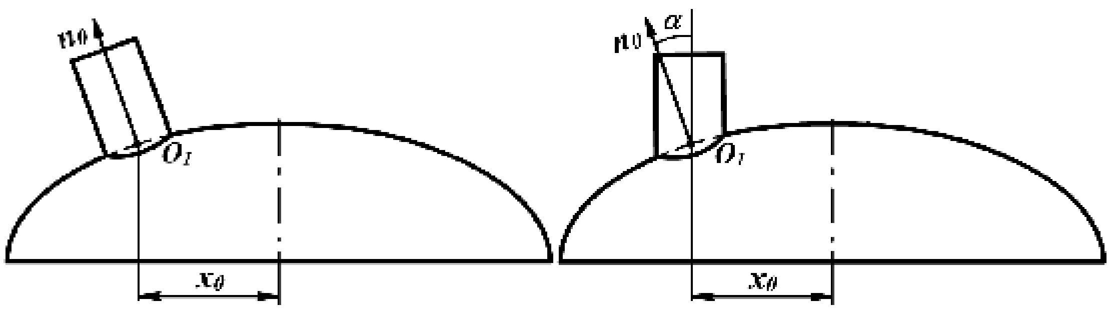

radial connection non-radial connection

b) ellipsoidal head with non-central nozzle

Fig.2. Typical nozzle connections in ellipsoidal head.

3. Finite element modeling

Stress analysis of the shell intersections was performed using the finite element method (FEM). Finite element modeling of the shell intersections includes the following specific features:

- the application of curvilinear coordinate systems of individual shells;
- the use of a modified mixed variational formulation and a shell-curved finite element with a special scheme for displacement and strain approximations;
- the use of a rational calculation algorithm with a minimum of coordinate transformations.

The finite element model of the ellipsoid-cylinder intersection uses shell-curved quadrilateral element ***ST4*** which was described in detail in Skopinsky (1999). The characteristics of the finite element were obtained using a modified mixed variational formulation and a transverse shear shell theory. The element nodal degrees of freedom, five at each node, are three pure displacements and two out of the plane rotation components in the curvilinear coordinate system of the reference shell surface. The approximations of displacement components and rotations, principal coordinates of the reference surface and shell thickness (in the case of a shell of variable thickness) are assumed by a bilinear interpolation in the local coordinate system of the element. A special scheme for the independent assumptions of the displacement, rotation and strain components for the mixed element model gives the improved characteristics of an element stiffness matrix in comparison with the usual displacement method. The mixed finite element formulation and element model were described in detail in Skopinsky (1999).

4. Computer program SAIS

The application of the curvilinear coordinate systems of individual shells makes it possible to use a rational calculation algorithm with a minimum of coordinate transformations. The numerical procedure used herein involves the determination of the geometric relationships for the intersection curve of the shell middle surfaces, which establishes the coupled relations between shell curvilinear coordinates and the matrix coordinate transformation. These nonlinear relationships in a parametric form can be written as follows

$$s_1 = f_1(\varphi_1), \qquad s_1 = f_2(\varphi_1), \qquad \varphi = f_3(\varphi_1) \tag{4.1}$$

where φ_1 is the angular (circumferential) coordinate of the nozzle (independent variable), s_1 is the axial (meridional) coordinate of the nozzle, s and φ are the meridional and circumferential coordinates of the ellipsoidal shell.

These relationships and transformation coordinate matrix are given in Skopinsky and Berkov (1994).

The finite element model of the shell intersection involves shell-curved quadrilateral elements for the approximation of the individual nozzle and ellipsoidal head. Irregular meshes of the finite elements on the shell surfaces, essentially for the region in the vicinity of the intersection curve, are used. An automatic mesh generation is carried out using the relationships (1) for nodal coordinates. For example, the finite element model of half of the ellipsoidal head with a non-radial and non-central nozzle is shown in Fig.3.

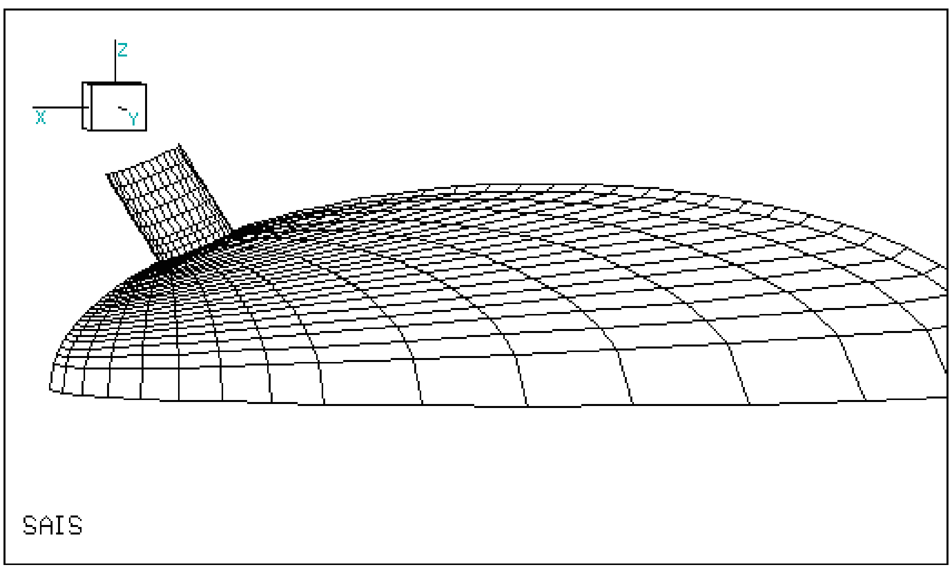

Fig.3. Finite element model of ellipsoidal head with nozzle.

The system of resulting equations with respect to the nodal displacement vector δ for the finite element model is obtained in the form

$$K\delta = F\,, \qquad K = \sum_e K^e\,, \qquad F = \sum_e F^e\,. \tag{4.2}$$

The stiffness matrix K^e and the load vector F^e of the element are obtained in the curvilinear coordinate system of every shell. In this case only the characteristics $\left(K^e, F^e\right)$ of the nozzle elements having nodes at the intersection curve are transformed to the coordinate system of the basic (ellipsoidal) shell using a block form of the element characteristics

$$K_{ij} = L_i^T K'_{ij} L_j, \qquad F_i = L_i^T F'_i$$
$$L_k = [\lambda_k, \lambda_k], \qquad k = i,\ j, \qquad 1 \le i, \qquad j \le 4 \tag{4.3}$$

where K_{ij} and F_i are the blocks of the element stiffness matrix and load vector respectively corresponding to the ***i***-th node at the intersection curve (blocks with a prime correspond to the nozzle coordinate system); L_k is the transformation matrix for the ***k***-th node of element (in case this node does not lie at the intersection curve, the matrix L_k is a unit diagonal matrix); the block λ_k is the matrix of coordinate transformation.

The nodal displacement vector of the nozzle elements having nodes at the intersection curve is obtained in the curvilinear coordinate system of the nozzle using the following transformation

$$\delta'_i = L_i \delta_i . \tag{4.4}$$

The stress components are determined at the nodal points of elements for the outside and inside shell surfaces. Moreover, the stress components of the ellipsoidal (basic) and cylindrical shells are separated for nodal points of the intersection curve.

The special-purpose computer program ***SAIS*** developed is employed for the numerical stress analysis of various models of the shell intersections. The ***SAIS*** (Stress Analysis in Intersecting Shells) is an object-oriented program providing a complete engineering environment (pre-processing, modelling, analysis and post-processing), and practical efficiency at relatively modest cost-time.

Program capabilities of the ***SAIS*** include analysis of such structural objects made of isotropic or anisotropic (composite) materials as follows:

- cylindrical, conical, spherical, ellipsoidal shells with nozzle
- pipe connections
- shell intersections with torus transition
- reinforced shell intersections
- mitred pipe bends.

5. Stress state features of ellipsoid-cylindrical intersection

The aim of this study is the stress analysis of nozzle connections in ellipsoidal heads under external loadings on the nozzle. In the general case, all applied forces and moments can be resolved in the three coordinate directions, i.e., they can be resolved into components P_x, P_y, P_z, M_x, M_y and M_z. The present stress analysis was concentrated on the action of four individually applied loads: axial force P_x, bending moments M_y and M_z, torsional moment M_x (Fig.4). Usually, these loadings cause the most significant stress concentration in shell intersection among the different external loading cases. Also, the stress components in the ellipsoidal head and cylindrical shell-nozzle are shown in Fig.4.

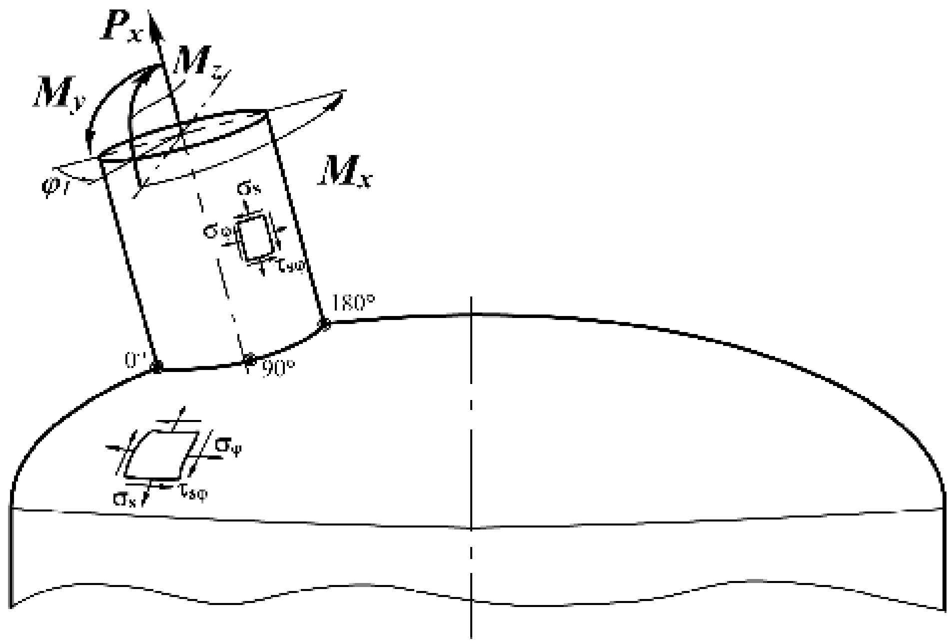

Fig.4. External loadings and stresses directions.

Main dimensions of a nozzle connection are shown in Fig.1. The important non-dimensional geometric parameters of the ellipsoidal-cylinder intersection are as follows

$$\bar{\boldsymbol{b}} = \boldsymbol{2b/D}, \qquad d/D, \qquad D/H \qquad (\text{or } d/h), \qquad h/H, \qquad \bar{x}_0 = \frac{2x_0}{D}, \qquad \alpha. \tag{5.1}$$

To examine the maximum effective stresses (by Tresca criterion) in shells of the nozzle connections under different loadings, the stress ratio was introduced in the following form

$$\bar{s}_{\boldsymbol{e}} = s_{\boldsymbol{e,max}}/s_0, \qquad \sigma_e = \sigma_1 - \sigma_3 \tag{5.2}$$

where σ_1 and σ_3 are the maximum and minimum principal stresses; σ_0 is the «nominal» stress of the connection.

Nominal stresses were defined for the basic stress state of the nozzle in accordance with the formulas

$$s_0 = \frac{P_x}{\pi dh} \quad \text{or} \quad s_0 = \frac{4M}{\pi d^2 h}, \qquad M = (M_x, M_y, M_z). \tag{5.3}$$

It can also be noted that relations (14) characterize the stress concentration effects in the nozzle.
The action of external loadings leads to a local stress state in the intersection region caused by the geometric discontinuity. The stress state is characterized by appreciable non-uniformity at the intersection region, considerable gradients of stress components, high stress concentration, particularly for thin-walled shells. Some general comments concerning basic features of the stress components and stress state of shells can be made basing on the stress analysis conducted for different external loading cases.

For the P_x, M_y and M_z loadings, some features of the stress state in the shells are common. The maximum effective stresses occur at the outside surface of the shells. Among the stress components in shells, the meridional stresses are of maximum value. There are primarily bending stresses both for the nozzle and the head. Contributions of the bending and membrane components into the circumferential stresses are approximately equal to each other.

For the P_x loading, the effect of the stress concentration is more significant than in the case of internal pressure loading, i.e., there is an appreciable increase of the maximum stresses for shells in the intersection region even at the small level of nominal stresses. The variations of normalized effective stress $\overline{\sigma}_e = \sigma_e / \sigma_0$ for the points of outside surfaces of the nozzle and head along the intersection curve are represented in Fig.5a. For comparison both dependences for radial and non-radial connections are illustrated. Non-radial and offset connections have significantly non-uniform distribution of the effective stresses on the intersection curve between the nozzle and the head.

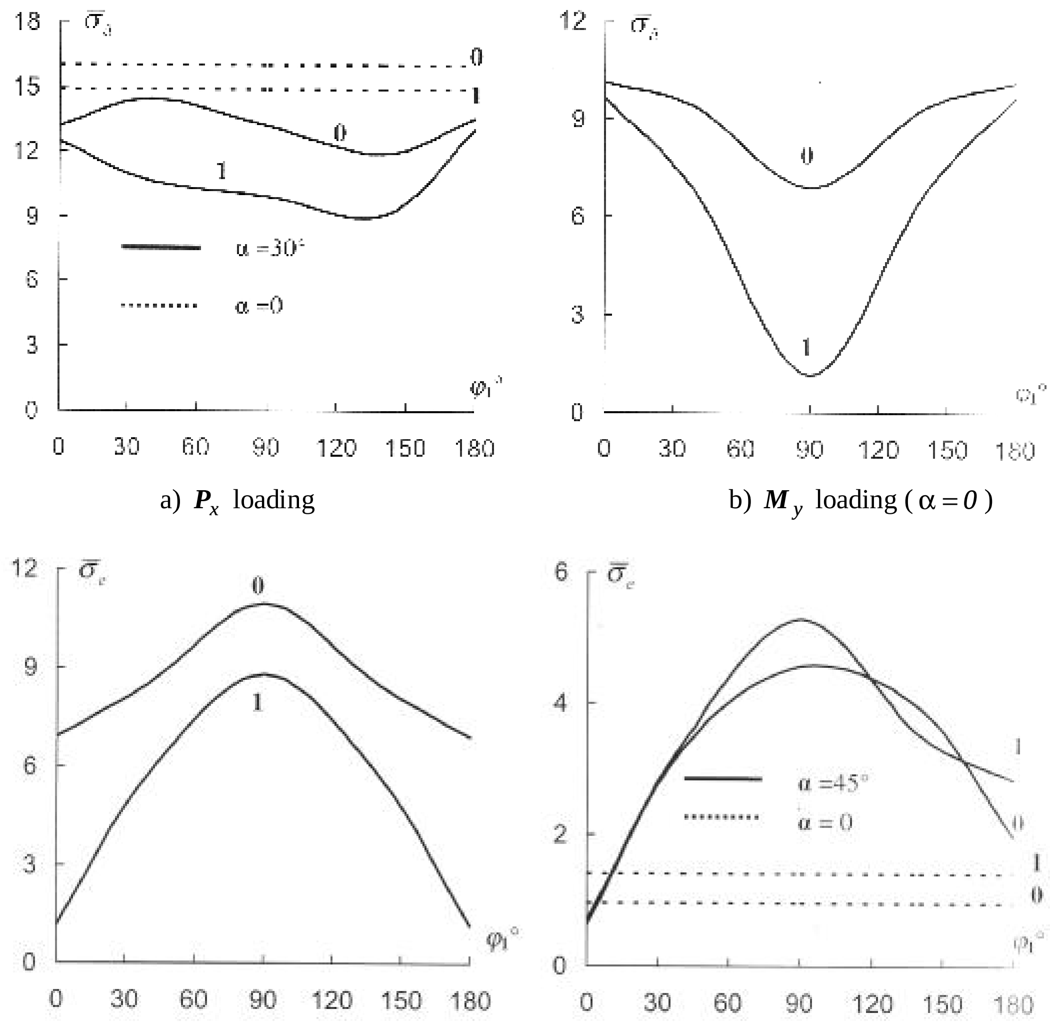

a) $\boldsymbol{P_x}$ loading

b) $\boldsymbol{M_y}$ loading ($\alpha = 0$)

c) $\boldsymbol{M_z}$ loading ($\alpha = 0$)

d) $\boldsymbol{M_x}$ loading

Fig.5. Variations of normalized effective stress on the outer surface of connections for different types of external loading (***0* – *nozzle*, *1* - *head***); ***d/D*** = *0,2*; ***D***/***H*** = *100*; 2***b/D*** = *0,5*; ***h/H*** = *1*; $\bar{x}_0 = 0$.

For the in-plane bending moment M_y loading, the stress concentration is lower than for the P_x loading. In this case the maximum stresses occur in the main plane at $\varphi_1 = 0^0$ and $\varphi_1 = 180^0$ and non-uniformity of the stress distribution along the intersection region is significant. Change of the deflection angle or offset parameter of the nozzle does not significantly influence the stress state in the shells. The distributions of effective stresses in the nozzle and head of radial connection are shown in Fig.5b.

For the out-plane bending moment M_z loading, the maximum effective stresses occur in the transverse plane of the connection (Fig.5c). For the non-radial and non-central connections, the contribution of the bending components into the circumferential stresses increases in comparison with its radial central counterpart.

For the torsional moment M_x loading of the radial central connections, the shear stresses are the basic components of the stress state; the stress concentration is practically negligible. However, the stress state in the shells changes significantly in the case of non-radial and non-central connections: the meridional and circumferential stresses are increased, effects of the stress concentration become significant, the maximum effective stresses in the nozzle and head occur in the transverse plane. The distributions of the effective stresses on the intersection curve for radial (dashed line) and non-radial (solid line) connections are given in Fig.5d.

6. Parametric study

In order to study the influence of geometric parameters (5) on the stress ratios in the shells of nozzle-head connections, a parametric analysis was conducted. The results of the analysis are presented in Figs 6-11 and in Tabs 1-5 for each of the individual loadings ($\overline{\sigma}_e^e$, $\overline{\sigma}_e^n$ – the stress ratios in the head and nozzle, respectively).

The parameter $2b/D$ determines relative depth of the ellipsoidal head. The value of this equal to 1 corresponds to a spherical head. The heads with $2b/D = 0.5$ (so-called standard ellipsoid head) are widely used in practical design. The influence of the parameter $2b/D$ on the maximum effective stresses in the shells of the radial nozzle connection is illustrated in Fig.6 for the P_x and M_y loadings. Similar results for the moments M_z and M_x are represented in Tab.1. Of course, a minimum value of the effective stresses in the shells is received for the sphere head.

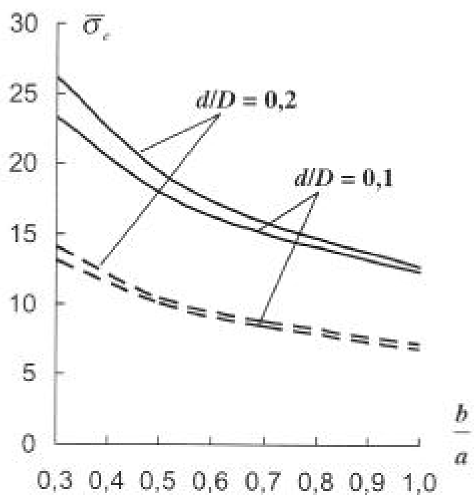

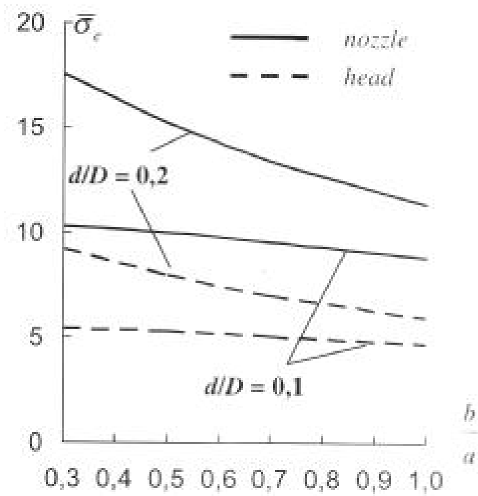

Fig.6. Influence of the parameter $\boldsymbol{2b/D}$ ($\boldsymbol{h/H}$ = *0,7*; $a = 0$; $\overline{x}_0 = 0$).

Table 1. Influence of the parameter $\boldsymbol{b/a}$ for $\boldsymbol{M}_z$ and $\boldsymbol{M}_x$ loadings $(\boldsymbol{h/H} = 0.7,\ \text{a} = 0)$.

		$\boldsymbol{M}_z(\bar{x}_0 = 0.5)$				$\boldsymbol{M}_x(\bar{x}_0 = 0)$			
	$\boldsymbol{b/a}$	*0.3*	*0.5*	*0.7*	*1*	*0.3*	*0.5*	*0.7*	*1*
$\boldsymbol{d/D} = 0.2$	$\bar{\sigma}_e^n$	*14.74*	*12.90*	*11.77*	*10.70*	*1.50*	*1.52*	*1.52*	*1.48*
	$\bar{\sigma}_e^e$	*7.69*	*6.62*	*6.00*	*5.53*	*0.71*	*0.72*	*0.72*	*0.73*
$\boldsymbol{d/D} = 0.1$	$\bar{\sigma}_e^n$	*9.88*	*9.41*	*8.99*	*8.55*	*1.50*	*1.51*	*1.51*	*1.50*
	$\bar{\sigma}_e^e$	*5.11*	*4.83*	*4.59*	*4.38*	*0.68*	*0.69*	*0.69*	*0.69*

Figure 7 and Tab.2 show the effect of the parameter d/D on the stress ratios in the head and nozzle. The influence of this parameter is more noticeable in the cases of the P_x, M_y and M_z loadings in comparison with the M_x loading. This tendency is observed due to an enlargement of the interaction area between the nozzle and the head as d/D increases.

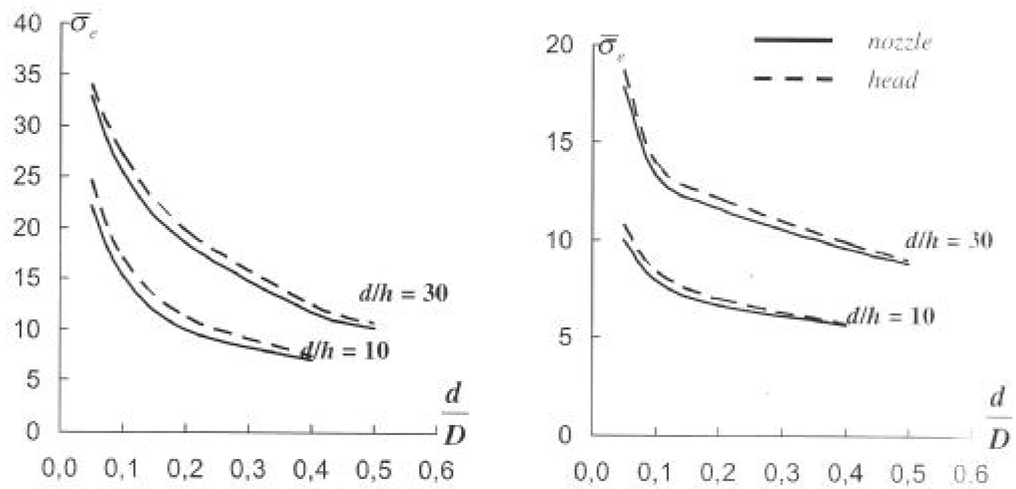

a) $\boldsymbol{P}_x$ loading b) $\boldsymbol{M}_y$ loading

Fig.7. Influence of the parameter $\boldsymbol{d/D}$ ($2\boldsymbol{b}/\boldsymbol{D}$ = 0,5; $\boldsymbol{h/H}$ = 1; a = 0; $\bar{x}_0 = 0$).

Table 2. Influence of the parameter $\boldsymbol{d/D}$ for $\boldsymbol{M}_z$ and $\boldsymbol{M}_x$ loadings $(2\boldsymbol{b/D} = 0.5,\ \boldsymbol{h/H} = 1,\ \text{a} = 0)$.

		$\boldsymbol{M}_z(\bar{x}_0 = 0.5)$				$\boldsymbol{M}_x(\bar{x}_0 = 0)$			
	$\boldsymbol{d/D}$	*0.05*	*0.10*	*0.20*	*0.40*	*0.05*	*0.10*	*0.20*	*0.40*
$\boldsymbol{d/h} = 10$	$\bar{\sigma}_e^n$	*9.64*	*7.57*	*6.70*	*4.07*	*1.67*	*1.67*	*1.66*	*1.60*
	$\bar{\sigma}_e^e$	*10.54*	*7.75*	*6.82*	*5.07*	*0.98*	*0.97*	*0.93*	*1.02*
$\boldsymbol{d/h} = 30$	$\bar{\sigma}_e^n$	*20.78*	*11.92*	*11.64*	*8.44*	*1.59*	*1.60*	*1.59*	*1.53*
	$\bar{\sigma}_e^e$	*22.31*	*11.19*	*10.06*	*8.79*	*1.00*	*0.99*	*0.96*	*0.99*

The influence of the parameter D/H is shown in Fig.8 and Tab.3. The results presented indicate that as D/H increases, an increase of the maximum stresses in the shells can be significant for the P_x, M_y, M_z loadings. In the case of the torsional moment loading a similar effect is obtained for non-radial nozzle connections only (see Tab.3).

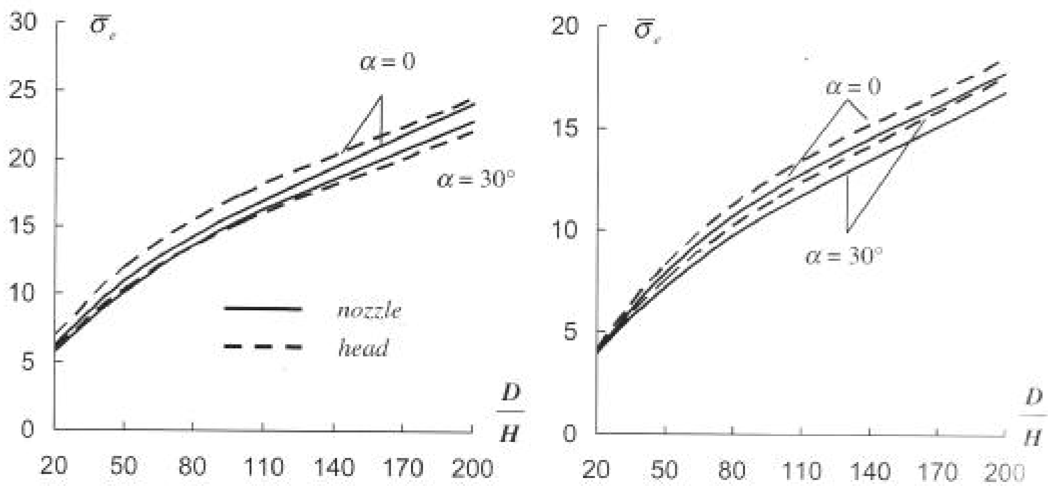

a) $\boldsymbol{P_x}$ loading b) $\boldsymbol{M_y}$ loading

Fig.8. Influence of the parameter ***D***/***H*** (***d***/***D*** = *0,2*; *2**b***/***D*** = *0,5*; ***h***/***H*** = *1*; $\bar{x}_0 = 0$).

Table 3. Influence of the parameter $\boldsymbol{D/H}$ for $\boldsymbol{M_z}$ and $\boldsymbol{M_x}$ loadings $(\boldsymbol{d/D} = 0.2, 2\boldsymbol{b/D} = 0.5, \boldsymbol{h/H} = 1, \bar{x}_0 = 0)$.

		$\boldsymbol{M_z}(\bar{x}_0 = 0.5)$				$\boldsymbol{M_x}(\bar{x}_0 = 0)$			
	$\boldsymbol{D/H}$	*20*	*50*	*100*	*200*	*20*	*50*	*100*	*200*
$a = 0$	$\bar{\sigma}_e^n$	*3.71*	*7.07*	*10.54*	*14.54*	*1.64*	*1.65*	*1.61*	*1.55*
	$\bar{\sigma}_e^e$	*3.72*	*7.26*	*10.88*	*14.90*	*0.97*	*1.01*	*1.02*	*1.02*
$a = 30^0$	$\bar{\sigma}_e^n$	*2.89*	*5.21*	*8.09*	*11.65*	*2.65*	*3.60*	*5.59*	*8.52*
	$\bar{\sigma}_e^e$	*3.01*	*5.39*	*8.19*	*11.78*	*2.13*	*3.72*	*5.78*	*8.69*

The parameter h/H defines the relative stiffness of the shells and significantly affects the maximum stress of the connection. Effects of this parameter on the stresses in the nozzle and head are different for the P_x, M_y, M_z loadings (Fig.9 and Tab.4). At the same time for the torsional moment M_x, the stresses in the shells increase as h/H increases (Fig.9c).

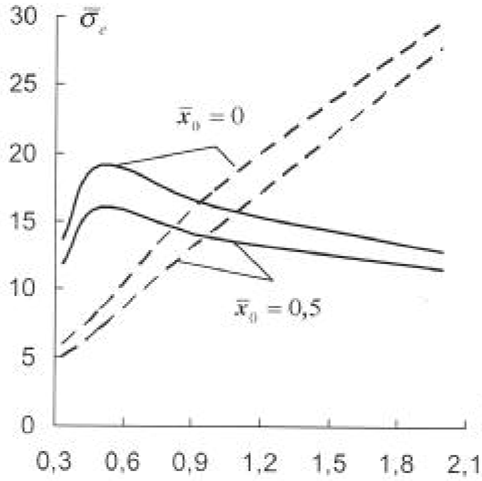

a) $\boldsymbol{P}_x$ loading

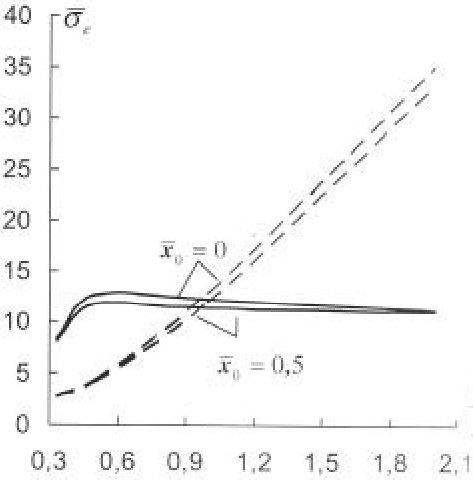

b) $\boldsymbol{M}_y$ loading

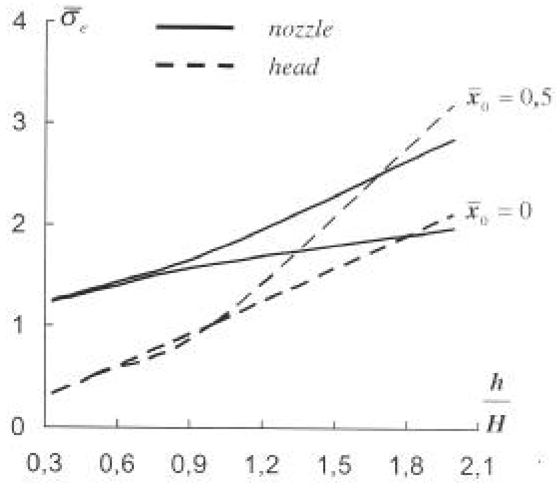

b) $\boldsymbol{M}_x$ loading

Fig.9. Influence of the parameter $\dfrac{h}{H}$ ($\boldsymbol{d}/\boldsymbol{D}$ = *0,2*; *2*$\boldsymbol{b}/\boldsymbol{D}$ = *0,5*; $\boldsymbol{d}/\boldsymbol{h}$ = *20*; *a* = *0*).

Table 4. Influence of the parameter $\boldsymbol{h}/\boldsymbol{H}$ for loading by moment $\boldsymbol{M}_z$ $(\boldsymbol{d}/\boldsymbol{D} = 0.2, 2\boldsymbol{b}/\boldsymbol{D} = 0.5, \boldsymbol{d}/\boldsymbol{h} = 20, \alpha = 0)$.

	$\bar{x}_0 = 0.3$				$\bar{x}_0 = 0.5$			
$\boldsymbol{h}/\boldsymbol{H}$	*0,33*	*0,50*	*1,00*	*2,00*	*0,33*	*0,50*	*1,00*	*2,00*
$\bar{\sigma}_e^n$	*8,07*	*11,14*	*11,11*	*8,49*	*7,77*	*11,21*	*10,54*	*6,99*
$\bar{\sigma}_e^e$	*2,66*	*4,90*	*11,69*	*24,17*	*2,57*	*3,73*	*10,88*	*22,07*

The influence of the angular parameter $\boldsymbol{\alpha}$ for the non-radial nozzle connections is shown in Fig.10. For the P_x, M_y, M_z loadings, a decrease of the maximum effective stresses as the angle α increases is more significant for the non-central connections. In the case of the torsional moment loading, the angle α affects the effective stresses in the opposite manner, i.e., the stresses in the shells increase as α increases.

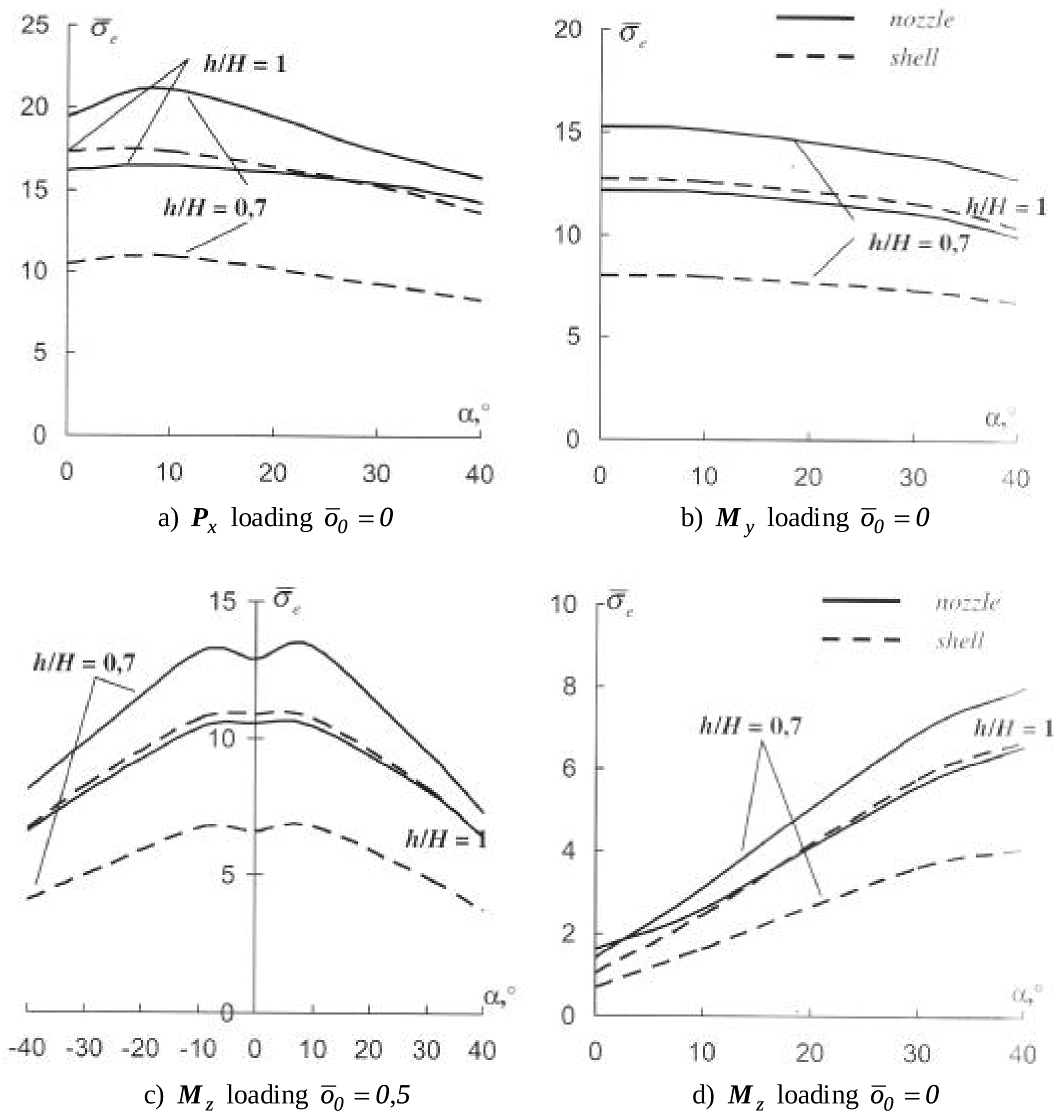

Fig.10. Influence of the angle *a* (***d***/***D*** = *0,2*; ***D/H*** = *100*; 2***b***/***D*** = *0,5*).

The influence of the parameter $\bar{x}_0$ for the external loadings is relatively small, the results are presented in Fig.11 and Tab.5 indicating opposite trends in the influence of the parameter $\bar{x}_0$ on the maximum effective stresses for the P_x, M_y, M_z and torsional moment M_x loadings, respectively.

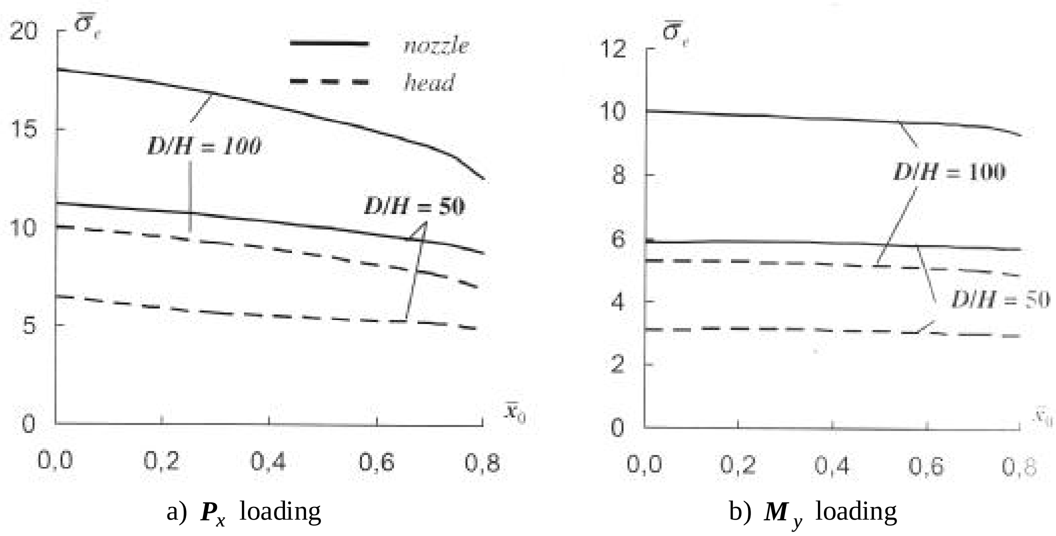

Fig.11. Influence of the parameter $\bar{x}_0$ ($\boldsymbol{d}/\boldsymbol{D}$ = *0,1*; $\boldsymbol{h}/\boldsymbol{H}$ = *0,7*; 2$\boldsymbol{b}/\boldsymbol{D}$ = *0,5*; *a* = *0*).

Table 5. Influence of the parameter $\bar{x}_0$ for $\boldsymbol{M}_z$ and $\boldsymbol{M}_x$ loadings $(\boldsymbol{d}/\boldsymbol{D} = 0.1, \boldsymbol{h}/\boldsymbol{H} = 0.7, \boldsymbol{2b}/\boldsymbol{D} = 0.5, \alpha = 0)$.

		$\boldsymbol{M}_z(\bar{x}_0 = 0.5)$				$\boldsymbol{M}_x(\bar{x}_0 = 0)$			
	$\bar{x}_0$	*0*	*0.3*	*0.7*	*0.8*	*0*	*0.3*	*0.7*	*0.8*
$\boldsymbol{D}/\boldsymbol{H} = 100$	$\bar{\sigma}_e^n$	*10.00*	*9.72*	*8.93*	*8.24*	*1.48*	*1.49*	*1.51*	*1.60*
	$\bar{\sigma}_e^e$	*5.29*	*5.06*	*4.49*	*4.17*	*0.68*	*0.68*	*0.69*	*0.70*
$\boldsymbol{D}/\boldsymbol{H} = 50$	$\bar{\sigma}_e^n$	*5.91*	*5.84*	*5.56*	*5.29*	*1.51*	*1.52*	*1.53*	*1.58*
	$\bar{\sigma}_e^e$	*3.10*	*2.96*	*2.74*	*2.63*	*0.66*	*0.67*	*0.67*	*0.70*

Conclusions

A procedure of the elastic stress analysis of nozzle connections in the ellipsoidal head subjected to external loadings is described. The numerical results of the stress analysis and parametric study performed are presented. Results show that it is necessary to pay more attention to the effective stresses in the shells in these loading cases. Although the stresses due to the external loadings are secondary stresses with respect to primary stresses from the internal pressure, these stresses should be taken into consideration in a complete stress analysis for nozzle connections of a pressure vessel.

Nomenclature

$\bar{b} = 2b/D$ – relative depth of ellipsoidal head
d/D – diameter ratio
d, h – mean diameter and thickness of nozzle
d/h – radius-to-thickness ratio for nozzle

D, b – mean diameter and depth of ellipsoidal head
D/H – diameter-to-thickness ratio for ellipsoid shell
h/H – thickness ratio
H – thickness of ellipsoidal head
l – length of nozzle
M_x – torsional moment applied at nozzle
M_y, M_z – bending moments at nozzle in main and transverse planes respectively
P_x – axial force at nozzle
x_0 – distance between nozzle and ellipsoid axes
$\bar{x}_0 = 2x_0/D$ – parameter of relative distance
α – angular parameter for nozzle axis
σ_0 – nominal stress for shell intersection
σ_e – effective stress $= \sigma_1 - \sigma_3$
$\sigma_e^{\max}$ – maximum effective stress for shell
σ_s, σ_φ – meridional and circumferential stresses in shell

References

Bijlaard P.P. (1955): *Stresses from local loadings in cylindrical pressure vessels*. – Trans. ASME, vol.77, pp.805-816.

Bijlaard P.P. (1957): *Computation of the stresses from local loads in spherical pressure vessels or pressure vessel heads*. – Welding Research Council Bulletin, No.34, March.

Chao Y.J. and Sutton M.A. (1985a): *Radial flexibility factors of nozzles in pressure vessel heads.* – J. Strain Anal. Eng. Des., vol.20, No.2, pp.87-92.

Chao Y.J. and Sutton M.A. (1985b): *Stress analysis of ellipsoidal shells with radial nozzle.* – Int. J. Pres. Ves. and Piping, vol.21, No.1, pp.89-108.

Chao Y.J. and Sutton M.A. (1985c): *Stress concentration factors for nozzles in ellipsoidal pressure vessel heads due to thrust loads.* – Int. J. Pres. Ves. and Piping, vol.19, No.1, pp.69-81.

Chao Y.J., Wu B.C. and Sutton M.A. (1986): *Radial flexibility of welded-pad reinforced nozzles in ellipsoidal pressure vessel heads.* – Int. J. Pres. Ves. and Piping, vol.24, No.2, pp.189-207.

Darevskiy V.M. (1964): *Determination of displacements and stresses in cylindrical shell under local loadings*. – Strength and Dynamics of Aeroengines, vol.1, pp.23-83.

Galletly G.D. (1959): *Bending of 2:1 and 3:1 open crown ellipsoidal shells*. – Welding Research Council Bulletin, No.59.

Galletly G.D. (1960): *Influence coefficients and pressure vessel analysis.* – Trans. ASME. J. of Eng. for Industry. August, pp.259-263.

Mashel N.G. (1977): *Strength analysis of ellipsoidal transitions in vessels and apparatus under internal pressure*. – Chemical and Petroleum Machine-building, No.6, pp.3-5.

Mershon J.L., Mokhtarian K., Ranjon G.V. and Rodabaugh E.C. (1984, 1987): *Local Stresses in cylindrical shells due to external loadings on nozzles – Supplement to WRC Bulletin 107 (Revision 1)*. – Revised Bulletin 297, August; Revised Bulletin 326, September 1987.

Skopinsky V.N. and Berkov N.A. (1994): *Stress analysis of ellipsoidal shell with nozzle under internal pressure loading*. – Trans. ASME. J. Pres. Ves. Tech., vol.116, No.4, pp.431-436.

Skopinsky V.N. (1999): *Theoretical analysis of composite shell intersections*. – Journal of Strain Analysis, vol.34, No.2, pp.107-116.

Skopinsky V.N. (2000): *Stresses in ellipsoidal pressure vessel heads with noncentral nozzle.* – J. Nucl. Eng. Des., vol.198, pp.317-323.

Skopinsky V.N. and Smetankin A.B. (2003): *Parametric study of pressure vessel head with offset nozzle*. – Int. J. of Pres. Ves. and Piping, vol.80, pp.334-343.

Gill S.S. (Ed.) (1970): *The stress analysis of pressure vessels and pressure vessel components*. – Oxford, p.592

Wichman K.R., Hopper A.G. and Mershon J.L. (1965, 1979): *Local stresses in spherical and cylindrical shells due to external loadings*. – Welding Research Council Bulletin, No.107, August, 1965, revised March, 1979.

Zemel V.A. and Fedenko G.I. (1974): *On strength analysis opening reinforcements in ellipsoidal heads of vessels and apparatus under internal pressure*. – Trudy LenNIIhimmash, No.8, pp.38-44.

Received: March 25, 2005

Revised: November 1, 2005